Available online at www.sciencedirect.com
ScienceDirect
Ultrasonics 48 (2008) 367–375
Ultrasonics
www.elsevier.com/locate/ultras

Flexible piezoelectric transducer for ultrasonic inspection of non-planar components

C.R. Bowen [a,*], L.R. Bradley [a], D.P. Almond [a], P.D. Wilcox [b]

[a] Materials Research Centre, Department of Mechanical Engineering, University of Bath, Bath, Somerset BA2 7AY, United Kingdom
[b] Department of Mechanical Engineering, University of Bristol, BS8 1 TR, United Kingdom

Received 16 November 2007; accepted 7 January 2008
Available online 14 February 2008

Abstract

This paper presents the fabrication and characterisation of a flexible ultrasonic transducer using commercially available PZT-5A piezoelectric fibers which are lapped to form rectangular piezoelectric elements. The key feature in the device construction is the inclusion of gaps between the piezoelectric fibers to ensure good flexibility in the plane normal to the fiber direction. The spatial response of the transducer ultrasonic output was assessed using acoustographic imaging. The flexibility of the transducer and its applicability in pulse-echo mode on curved sections was demonstrated by testing on a 38 mm diameter steel rod. The transducer response was found to be broad band and highly non uniform but good pulse-echo performance was achieved at 5 MHz.

PACS: 43.38.Fx

Keywords: Flexible; Transducer; Piezoelectric; NDE

1. Introduction

For ultrasonic non-destructive evaluation (NDE) of curved, irregular or complex shaped profiles there is a need for flexible transducers that are able to conform to the profile of the component being inspected. Traditional dense, monolithic piezoelectric ceramics, such as lead zirconate titanate (PZT), are generally unsuitable for such applications as they are inherently brittle and are of high stiffness. In order to produce a flexible transducer a variety of methods have been attempted. Hayward et al. have considered the development of a flexible transducer at a theoretical and experimental level [1–6]. One approach was to embed piezoelectric platelets with high aspect ratio in a polymer matrix so that each platelet can be treated as a pure thickness mode device; although a high width to height aspect ratio can lead to reduced flexibility [2]. A copper-polyimide printed circuit board was used to interface with the material [3] and an interdigitated electrode was used to generate Lamb waves [5]. One possible danger of a piezoceramic–polymer configuration is that continual flexing of the material can lead to debonding and delamination of array elements [6]. Another approach to generate a flexible transducer is to randomly disperse isolated piezoelectric particles in a polymer matrix to form a 0–3 composite [7]. However the low electromechanical efficiency, relatively low piezoelectric coefficients [7] and low dielectric constant may limit their use in active applications [1].

The French atomic energy commission [8] developed a different approach to design a transducer that could conform to the profile of cooling pipes of pressurised water reactors. The transducer was a flexible phased array contact transducer which consisted of 24 individual ultrasonic transducers [9,10]. The elements were mechanically joined and assembled with cables and helical springs to form a flexible array that could make contact to an irregular surface. Kobayashi et al. [11] developed of flexible ultrasonic

* Corresponding author. Tel.: +44 1225 383660.
E-mail address: c.r.bowen@bath.ac.uk (C.R. Bowen).

0041-624X/$ - see front matter © 2008 Elsevier B.V. All rights reserved.
doi:10.1016/j.ultras.2008.01.006

transducer which consisted of the stainless steel base metal foil, a PZT piezoelectric ceramic film and a top electrode of silver paste. The thin metal foil served as a substrate and base electrode and could be deformed to conform to the shape being inspected. The PZT was applied using a sol–gel process and the porosity in the film was thought to increase the flexibility of the piezoelectric. The transducer could operate at high temperatures (160 °C) and was evaluated on a curved pipe section. The final method of achieving flexibility is to replace the ceramic with a piezoelectric–polymer [12]. However, like the 0–3 composites, these can be rather poor transmitters of ultrasound [2,3]; although they possess a number of advantages for high frequency medical ultrasound (>15 MHz) [12].

While the piezoelectric ceramic element can often be made flexible, one problem is debonding of the electrode from the surface of the piezoelectric material during continued flexing to high curvature. The aim of this paper is to report on the manufacture of a simple, robust and low cost flexible transducer using commercially available piezoelectric fibres and to present results that demonstrate its applicability in pulse-echo mode on curved sections.

2. Basic transducer structure

The active elements of the flexible transducer were cylindrical 800 μm diameter PZT-5A fibres [13] that had flats ground onto them such that they possessed two parallel opposite faces. The ground fibres were subsequently placed in parallel with a small, 0.8 mm, air gap separating them. The air gap allowed flexibility of the transducer normal to the fibre direction. This is in contrast to commercially available interdigitated fibre transducers, such as the macro fibre composite where the curvature is parallel to the fibre axis. Although it is possible to fill the air gap between fibres with a polymer to form a conventional 2–2 configuration, this was avoided since bending of an alternating PZT/polymer/PZT configuration normal to the fibre axis leads to curvature of the lower stiffness polymer (Fig. 1a). This can lead to debonding at the electrode–polymer interface (Fig. 1a) and ultimately failure of the electrode from adjacent ceramic fibres. Similarly, there could be debonding of the PZT–polymer interface. By maintaining an air gap between the fibres, only the electrode is subjected to bending and there is no bending of the ceramic-electrode interface to initiate debonding (Fig. 1b).

The electrodes were copper-coated Kapton polyimide films with the electrode structure and area formed by etching to remove the copper. Electrodes were attached to the piezoelectric elements using silver loaded epoxy adhesive. The structure and assembly of the transducer will now be described in detail.

3. Device construction and characterisation

3.1. Fibre thickness

The transducers were designed to operate at a frequency of 3.3 MHz so that their output signal could be examined using an acoustography ultrasound system [14] that operates resonantly at 3.3 MHz. The thicknesses of the fibres were selected such that the series resonant frequency, f_s, would be ~3.3 MHz. For a piezoelectric bar (or square fibre) in transverse length mode, the compliance at constant electric field (or short circuit compliance), S_{11}^E, is related to the density of the material ρ, the series resonance frequency f_s and the transverse length l by Eq. (1) [15].

$$l = \frac{1}{\sqrt{4\rho f_s S_{11}^E}} \tag{1}$$

For bulk PZT-5A the relevant material properties are, $\rho = 7750\ \mathrm{kg\,m^{-3}}$ and $S_{11}^E = 16.410^{-12}$ Pa [16], although Nelson et al. [17] have shown differences between bulk and fibre properties. In order for f_s to be 3.3 MHz the thickness required for the fibre is 420 μm.

3.2. Fibre grinding and lapping

Fig. 2a shows fibres attached to a plate using a wax prior to grinding. After grinding and lapping to the appropriate thickness, the fibres were removed from the plate by reheating the plate to melt the wax. After grinding both faces of the fibres, any wax on the ground surfaces was carefully removed using a scalpel. However, the wax on the edges of the fibres was left in place to act as a mask to prevent an electrical short developing during the application of a gold electrode to the ground faces. Fig. 2b and c show secondary

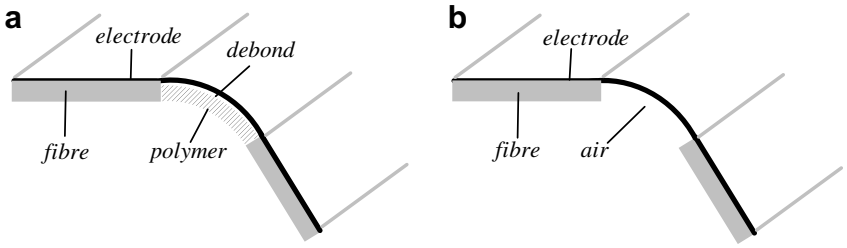

Fig. 1. Cross-section of flexible tranducer during bending (bottom electrode layer not shown for clarity) (a) bending of polymer–electrode interface initiating debonding (b) air gap between fibres ensures no electrode interface is subjected to bending.

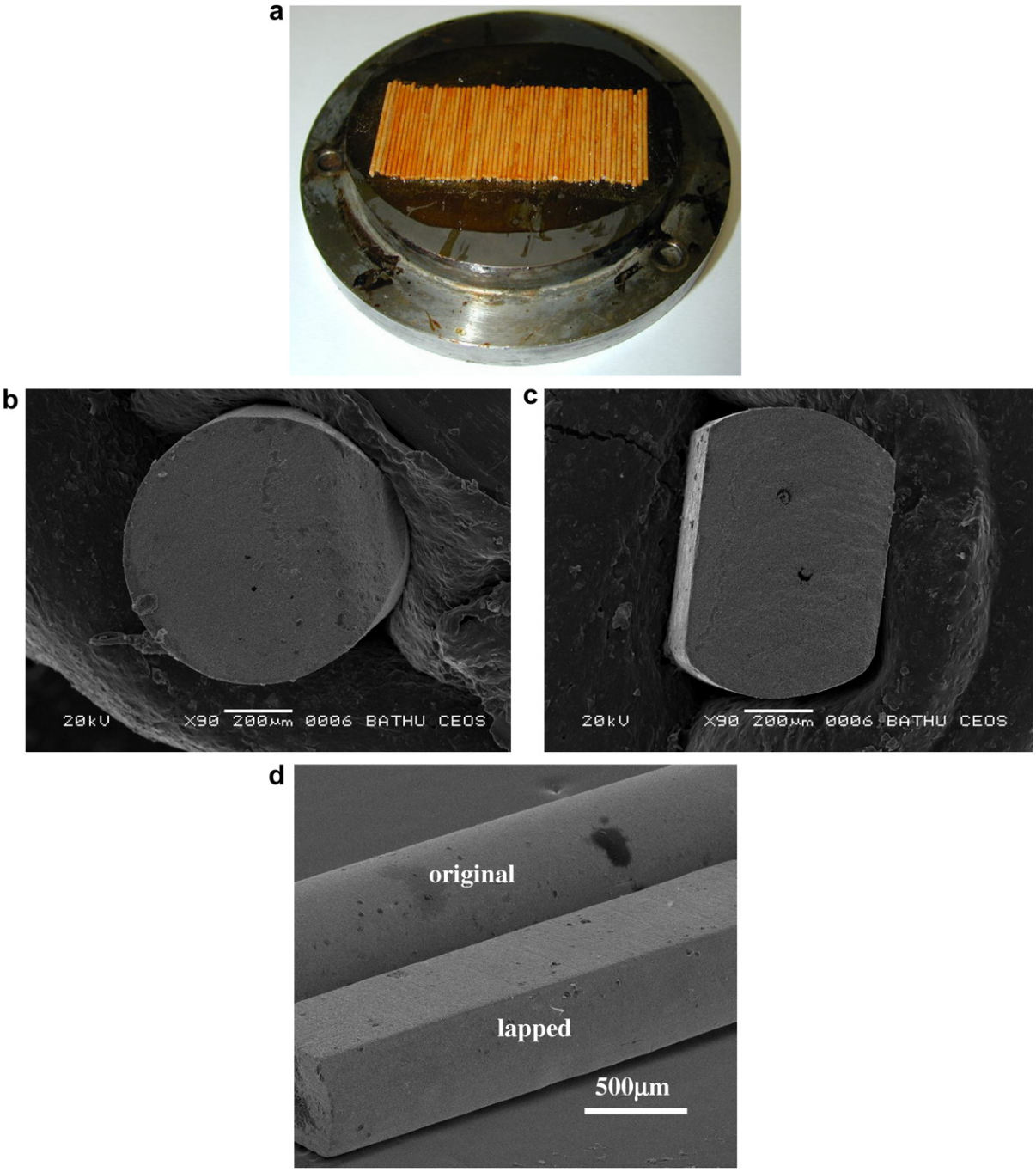

Fig. 2. Element fabrication (a) grinding of fibres attached to plate (b) initial fibre (c) lapped fibre (d) comparison of original and lapped fibre.

electron scanning electron micrographs of the initial fibre (diameter 800 μm) and the fibre lapped to 420 μm, respectively. The width of the ground fibre remains at 800 μm. Fig. 2d shows a section along the length of a wax free lapped fibre, along with the non-lapped (original fibre).

3.3. Application of fibre electrodes

A variety of methods were examined to apply electrodes to the fibres. The two main electrode coating methods are shown in Table 1. Gold electrodes were deposited on Type A fibres by chemical vapour deposition (CVD). Type B fibres were initially gold sputter coated on each of the surfaces that required electroding. After the thin gold sputter coating was applied to both surfaces the electrode layer was subsequently made thicker by depositing an additional

Table 1
Types of gold coatings applied as electrodes to both sides of the fibres whose impedance characteristics are shown in Fig. 3

Fibres	Type of gold coating applied as electrodes
Type A	One CVD cycle
Type B	One 5 min sputter coat then one CVD cycle

CVD gold coating. This was necessary since a sputter coated electrode is very thin, <1 μm and was easily worn from the fibre face during transducer manufacture.

Although the sputtering and the CVD processes resulted in the non-ground edges of the fibres being coated with gold, thus forming a short circuit between electrodes, the presence of the wax on the sides of the fibres allowed the gold to be easily removed by removing the wax with a scalpel blade. Following application of electrodes, each fibre was checked for short circuits between the electrodes using a multimeter.

3.4. Fibre poling

Electroded fibres were corona poled at a temperature of 100 °C using a potential difference of 11 kV and a base to needle distance of 15 mm, with the fibres left to cool at room temperature in the presence of the electric field. Before poled fibres were incorporated into a flexible device, their d_{33} values were measured using a piezometer (Take Control Piezometer System PM25). Poling the fibres resulted in measured d_{33} coefficients of 150–200 pCN^{-1}, which is lower than that of monolithic PZT-5A of the same composition (~350 pCN^{-1} [16]). The same fibres, when poled along their length had achieved a d_{33} of ~260 pC N^{-1}[17]. An explanation for the difficulty in achieving d_{33} in excess of 200 pCN^{-1} when poling though the thickness may be that a preferred grain orientation exists in the fibres due to their processing route (extrusion). Any fibres with $d_{33} < 165$ pCN^{-1} were re-poled and discarded if still below this after a second poling treatment.

3.5. Measurement of impedance characteristics versus frequency

Before manufacturing the flexible transducer using the poled fibres, the impedance spectrum of individual fibres was measured using an impedance analyser (Agilent Technologies Precision Impedance Analyser 4294 A) over a frequency range of 40 kHz to 6 MHz at an excitation potential of 500 mV. This range enabled the presence of an impedance drop at the thickness mode resonant frequency to be confirmed, as well as allowing lower and higher frequency resonance modes of the fibres to be observed. The impedance characteristics of two typical fibres (Type A and B) are shown in Fig. 3. It can be seen that for Type A fibres, whose electrodes are applied with a single CVD cycle and no sputtering, only a very slight resonance can be observed at ~2 MHz (see Fig. 3a). Fibres with electrodes formed with a sputter coat of gold, followed by a single CVD cycle (Type B) exhibited a much sharper resonance response (Fig. 3b). The impedance of the fibres of Type A is also higher than Type B. This suggests that the absence of a sputter coating prior to the gold CVD cycle results in higher measured impedance, which appears to be due to the sputter coating forming a better bond with the fibre than the CVD coating due to the gold ions used in sputter coating possessing higher energies. The use of a gold sputter coating prior to the CVD coating was therefore used when applying gold electrodes to all the fibres in the flexible transducer.

A notable feature in Fig. 3b is that the most prominent resonance is at ~1.9 MHz and the desired resonance at ~3.3 MHz (fundamental thickness mode) is smaller. This lower frequency resonance corresponds to the fundamental frequency of lateral vibrational modes across the ~0.8 mm wide fibres, calculated to be ~1.8 MHz using Eq. (1). The resonances above 3.3 MHz correspond to the excitation of harmonics of the approximately rectangular cross-section fibres. The use of high aspect ratio square platelets by Hayward et al. [1] ensures that the thickness and width resonant modes are widely separated, however such a structure requires a polymer matrix which can initiate electrode debonding.

3.6. Device electrodes and their attachment to piezoelectric elements

A copper-coated Kapton film was used to form the encapsulation of the fibres and the electrode contact to

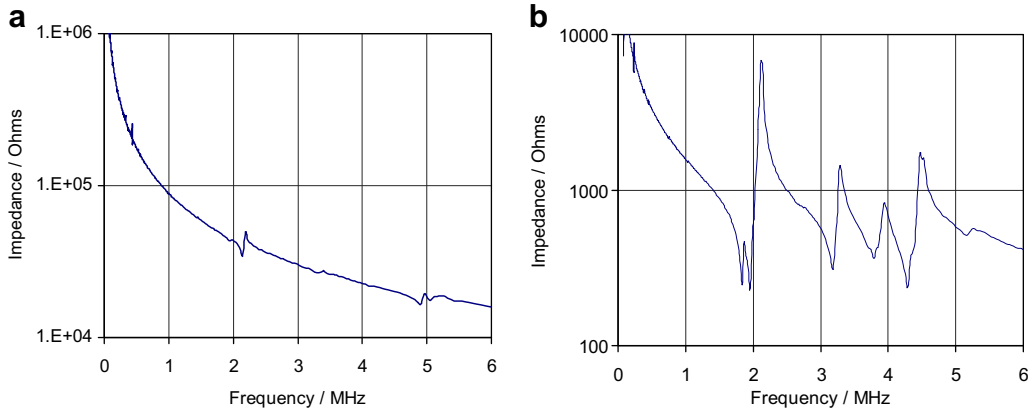

Fig. 3. Impedance characteristics of fibres at an excitation potential of 500 mV over a frequency range of 0–6 MHz. (a) One CVD cycle and (b) 5 min sputter coat and one CVD cycle.

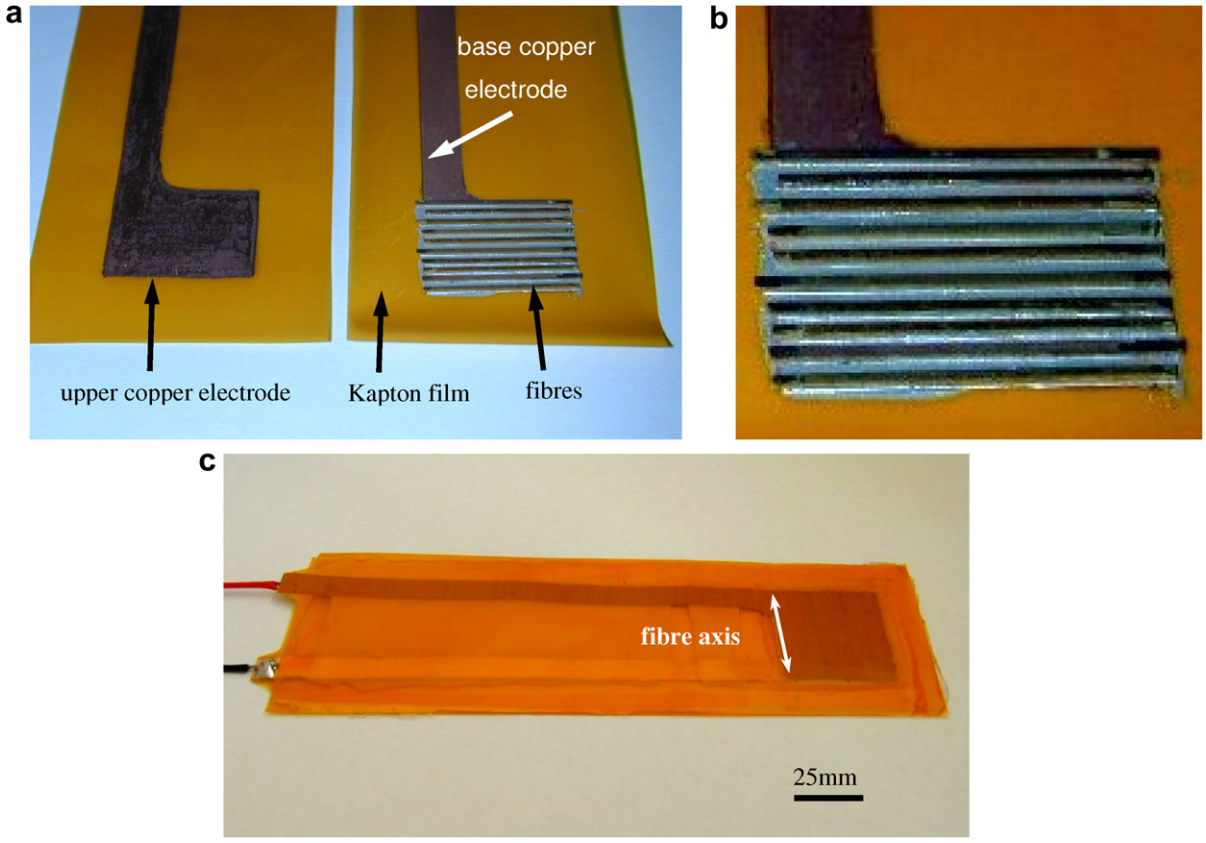

Fig. 4. Transducer fabrication. (a) Kapton film after etching with piezoelectric fibres attached to one side of device (b) enlargement of fibre area (c) completed device with fibre direction indicated.

the fibres. To prevent the device being shorted out by the copper coating, the copper was removed from the film, except in areas where it was required to form the device electrodes and electrical connector strips (Fig. 4a). This was accomplished by initially marking the area where the device electrodes were required using an etch-resistant pen. The film was then placed in an acidic ferric chloride etch, which removed the exposed copper coating leaving copper device electrodes in the desired position. The etch-resistant ink was finally removed using acetone.

The poled gold coated fibres were attached to the copper film using silver loaded conductive epoxy glue (Circuit Works Conductive Epoxy CW2400). To avoid the conductive glue flowing into the region between the fibres, thereby creating a short circuit between the two device electrodes, a very thin layer of the conductive glue was used. This was achieved using a razor blade to spread the glue over the surface of the first device electrode. Non-contact profilometery using a Proscan 2000 with a chromatic sensor S5/03 (0.01 μm resolution) determined the epoxy thickness to be 40–45 μm.

The piezoelectric fibre elements were then placed in their desired positions using tweezers and microscope slides placed over them upon which a small mass (250 g) was placed and the glue left to dry. Fig. 4a and b show the fibres attached to one electrode. Once this had dried, the mass and slides were removed and the conductive glue was applied to the second electrode and attached to the fibres in the same manner. Care was taken to prevent excess air becoming trapped between the two Kapton sheets during this process. Microscope slides were placed upon the top of the device and gently pressed to ensure that the device was flat and that the second device electrode was in contact with the piezoelectric elements. Excessive force was avoided to prevent the silver glue being squeezed between the device electrodes and causing a short circuit between them. After the glue had dried, wires were soldered to the ends of the electrical connector strips to form the com-

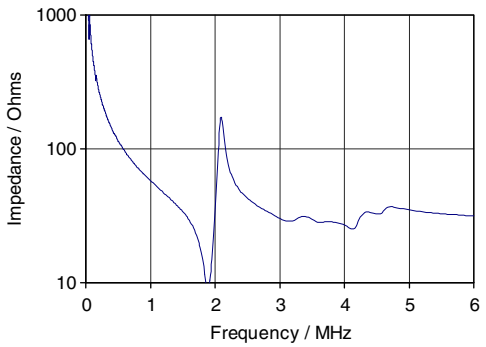

Fig. 5. Impedance characteristics of fibre device at an excitation potential of 500 mV.

pleted device (Fig. 4c). The flexibility of the device was good if flexed normal to the fibre direction.

Fig. 5 shows the impedance characteristics of the completed transducer over the frequency ranges 0–6 and 0–0.6 MHz. The most notable feature is the resonance just below 2 MHz, which is also exhibited by the individual fibres (Fig. 3). However the peaks between 2 and 5 MHz exhibited by the individual fibres are smaller for the small fibre device. The impedance of the device is also lower than that of the individual fibres.

4. Acoustography imaging

The completed transducer device was imaged using an acoustography system [14] to qualitatively assess its output. Acoustography is a broad-area ultrasonic imaging technique. It employs an acousto-optic imager formed by a layer of ultrasound-sensitive liquid crystal that enables large areas to be imaged instantaneously. The imager is a device that depends on a resonant interaction between ultrasonic waves and the liquid crystal film. The thickness of the film sets the resonant frequency; to 3.3 MHz in the system used here. The complete acoustography inspection system comprises the acousto-optic imager and a large area piezoelectric transducer sound source positioned in a water immersion tank, separated from each other by about 15 cm. A part to be inspected is placed in the water between the transducer and the imager to produce an acoustic shadow image that is comparable to a transmission C-scan image. The system used here had a 65 mm square piezoelectric transducer that generated 3.4 MHz ultrasound and a circular 75 mm diameter acousto-optic imager.

The flexible transducer was suspended by its connecting wires inside the acoustography system immersion tank approximately 5 cm in front of the acousto-optic imager. The acoustography system sound source was activated to form the shadow image of the flexible transducer shown in Fig. 6a. This provided a useful means of defining the position of the flexible transducer and the active area, which could be referred back to in subsequent tests.

Following the above, the acoustography system sound source was switched off and the flexible transducer was operated at frequencies between 3.2 and 3.5 MHz at voltages between 40 and 100 V (peak to peak). The acoustographs of the transducer show good emission at 80 V and 100 V over the region occupied by the fibres. Fig. 6b–c show the acoustography images for 100 V condition at 3.4–3.5 MHz. It can also be seen that the brightest part of the device is the upper half of the piezoelectric region. One possible explanation for this is that the bonding of the electrodes is superior in this region. During construction, fibres in this region were placed down before those

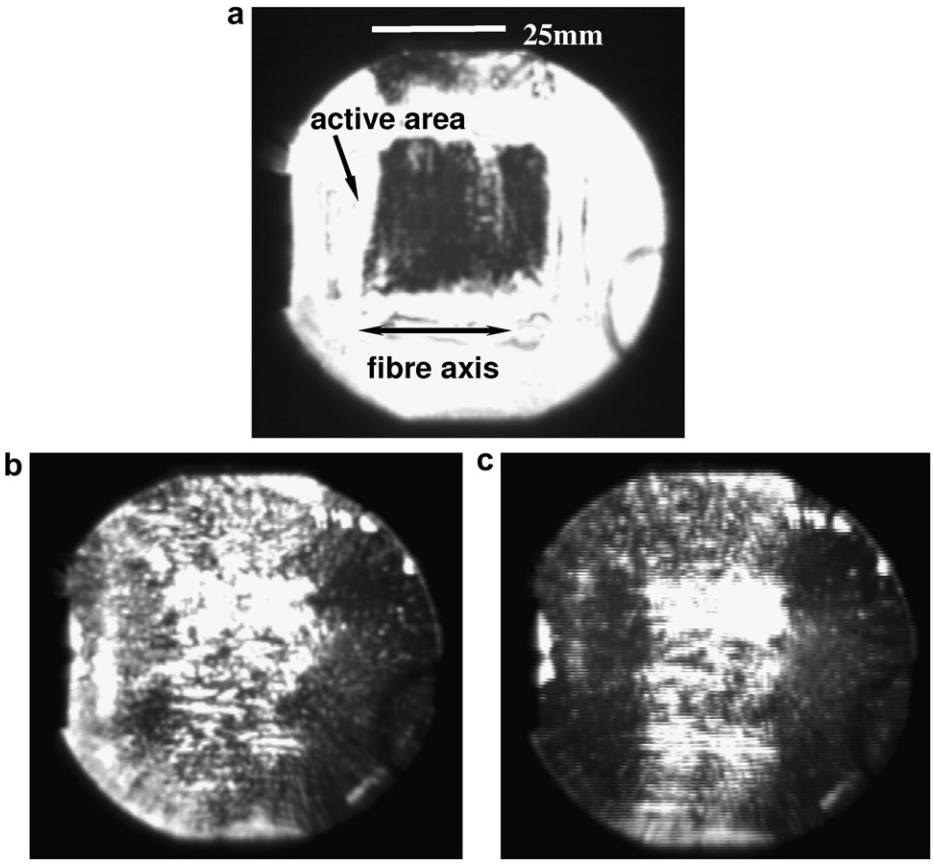

Fig. 6. Acoustographs of fibre device at an excitation voltage of 100 V. (a) Back lit (to show position of device); (b) 100 V, 3.4 MHz and (c) 100 V, 3.5 MHz.

in the lower region, which may have resulted in a superior bond since the adhesive exhibited a slight but noticeable degree of hardening during the placement of the fibres. For devices with larger numbers of fibres, the fibres could be laid down in three or four batches according to the size of the device.

5. Transducer testing in pulse-echo mode

The flexible transducer was tested for its pulse-echo performance on a non-planar test piece in the form of a 38 mm diameter steel rod, as shown in Fig. 7. A 10 mm diameter hole was drilled along the axis of the rod to provide a reflecting surface for ultrasound generated by the transducer in the rod. The flexible transducer was wrapped around the rod as shown in the figure.

Acoustic coupling between the transducer and the rod was achieved using commercial coupling gel. The pulse–echo performance of the transducer was first assessed using a MATEC 6600 pulsed oscillator receiver unit. This system employs a gated pulsed oscillator to generate drive pulses, of ~1 μs width, at a user defined central frequency and a tuned amplifier in its receiver. The clearest A-scans obtained from the transducer coupled to the test rod were found at frequencies ~5 MHz and an example is shown in Fig. 8. This can be seen to comprise two pulse-echo trains labelled A and B. The echo train A has an echo spacing of ~4.5 μs which is in excellent agreement with that expected for a pulse-echo reflection from the 10 mm diameter hole, insert A Fig. 8, longitudinal wave velocity in steel is 5810 ms^{-1}. The echo train B has an echo spacing of about 16.5 μs which corresponds with the four skip acoustic path around the central hole indicated in insert B Fig. 8. These results show that a clear reliable pulse-echo response can be obtained from the flexible transducer applied to a high curvature part.

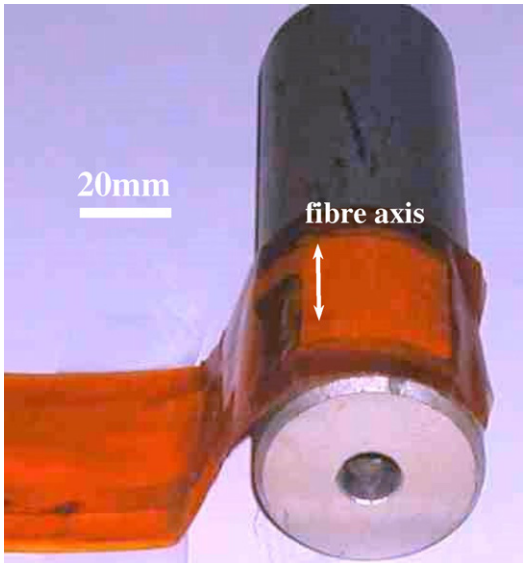

Fig. 7. Flexible transducer attached to steel cylinder.

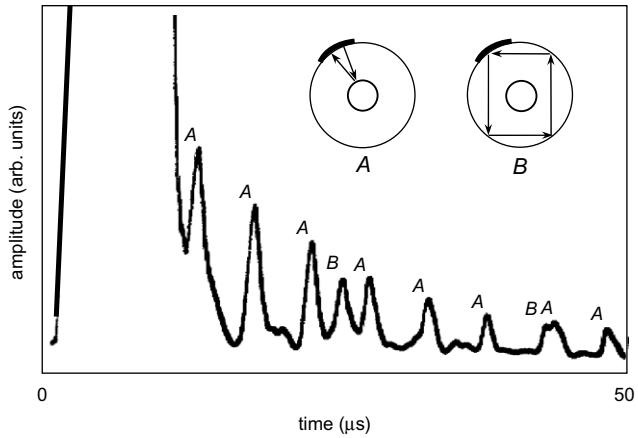

Fig. 8. Pulse-echo response obtained from the flexible transducer applied to a 38 mm diameter steel rod containing an axially drilled 10 mm diameter hole.

In order to asses the frequency spectrum of the transducer it was connected to an ultrasonic pulser–receiver (Panametrics 5072PR). The pulse repetition frequency of 100 Hz and a receiver amplifier gain of 29 dB were used. The built in low pass filter in the pulser–receiver was used to filter out frequencies above 10 MHz in the received signal. Additional settings on the pulser–receiver were transmit pulse energy level 1 and damping level 3. The pulser–receiver outputs a broadband pulse to the transducer. The received signal from the transducer after amplification in the pulser–receiver was recorded using a digital oscilloscope (TiePie Handyscope HS3), sampling at 50 MHz with 12 bit resolution. No averaging was performed on the received signal.

The received time-domain signal (A-scan) and its frequency spectrum are shown in Fig. 9a and b, respectively. It can be seen from the frequency spectrum that the transducer is broadband in that the received signal has energy content up to a frequency of around 9 MHz. However, its frequency response is not at all flat and contains multiple resonances, the strongest of which is at around 2 MHz. For this reason, the raw time-domain signal is inadequate for NDE usage in conventional pulse-echo (or pitch-catch) configurations. However, the signal quality can be significantly improved by filtering. Here filtering was performed in post-processing using Matlab, but the same effect could be readily achieved using either a narrowband toneburst signal on transmission or an analogue bandpass filter in reception. The first filter employed was tailored to target the resonant peak in transducer response at 2 MHz and used a Gaussian frequency window with −40 dB points at 1 and 3 MHz. This filter is superposed on the frequency spectrum in Fig. 9b and the resulting A-scan is shown in Fig. 9c. Although there is some structure present in the A-scan, the pulses are too long to be clearly resolved from each other, indicating that the 2 MHz resonance is too narrowband to be exploited directly.

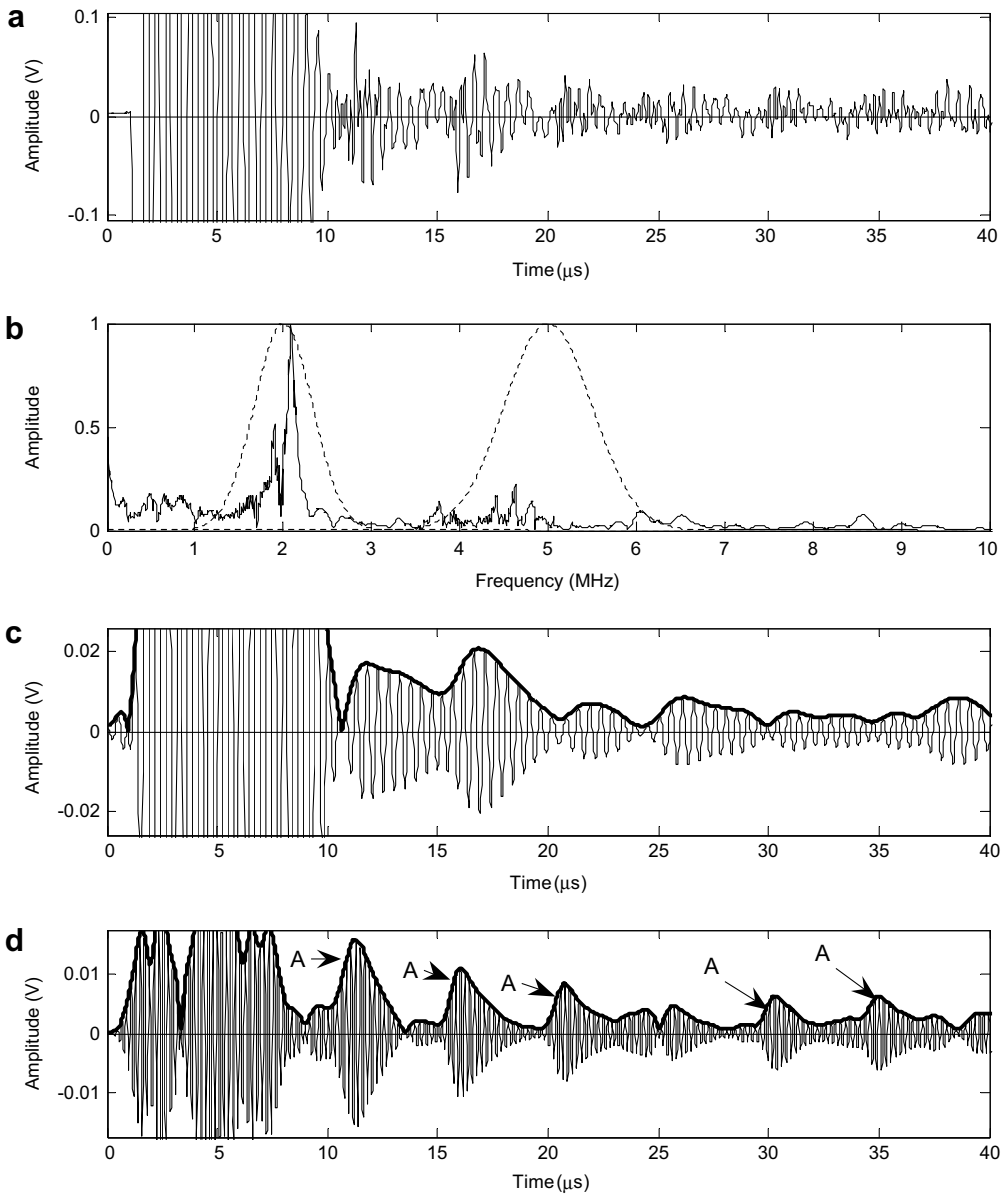

Fig. 9. (a) Raw A-scan obtained from the flexible transducer applied to a 38 mm diameter steel rod containing an axially drill 10 mm diameter hole; (b) frequency spectrum of raw A-scan showing positions of Gaussian bandpass filters; (c) A-scan after applying Gaussian bandpass filter from 1 to 3 MHz; (d) A-scan after applying Gaussian bandpass filter from 3.5 to 6.5 MHz. In (c) and (d) the gray lines are the RF signals and the bold black line is the (Hilbert) envelope of the signal.

The filter was then changed to target the higher frequency portion of the spectrum around 5 MHz. Again a Gaussian frequency window was used, this time with −40 dB points at 3.5 and 6.5 MHz. This filter is also superposed on the frequency spectrum in Fig. 9b and the resulting A-scan is shown in Fig. 9d. This A-scan has many similarities to that obtained using the MATEC 6600 system, shown in Fig. 8. The train of echoes (labelled A in the figure) is again clearly visible with a spacing of ~4.5 μs.

The ultrasonic frequency spectrum, Fig. 9b shows a strong peak at ~2.2 MHz whilst the impedance spectra of the fibres and the whole transducer showed fundamental resonances at ~1.8 MHz, Figs. 3b and 5. In addition, the group of peaks in Fig. 9b between ~3.7 MHz and 5 MHz appear to correlate with the higher frequency resonances in Fig. 3b moved to higher frequencies. A difference between the impedance spectroscopy measurements and the ultrasonic measurements is the voltage used in the two cases; 500 mV for impedance spectroscopy and 100 V for the ultrasonic measurements. It is known [18] that the electric fields applied to ferroelectrics, particularly 'soft' compositions such as PZT5A, can alter the polarisation state as a result of extrinsic contributions (domain motion), leading to changes in elastic and piezoelectric coefficients. These results show that a clear reliable pulse-echo response can be obtained from the flexible transducer applied to a high curvature part.

6. Conclusions

This work has demonstrated the manufacture of a flexible piezoelectric transducer utilising piezoelectric fibres ground to form rectangular fibres of the appropriate thickness. An air gap between the fibres enables good flexibility normal to the fibre direction and limits the potential for debonding of the active ceramic phase from the electrode when subjected to bending. The manufacturing process can be significantly simplified by directly fabricating rectangular rods of the required dimension. Such a process has already been developed on a commercial scale for macro fibre composite actuators, although these devices have interdigited electrode structure and since the axis of curvature is along the fibre direction there is a lesser degree of conformability. To ensure good contact between the electric and active element a gold sputter coating prior to the application of a gold CVD coating improved the measured impedance characteristics of the fibres, compared to the application of a gold CVD coating alone.

The flexibility of the transducer and its applicability in pulse-echo mode on curved sections was demonstrated by testing on a 38 mm diameter steel rod. The results demonstrate that a clear reliable pulse-echo response can be obtained from the flexible transducer applied to a high curvature part. The transducer was found to have a broad band highly non uniform frequency response dominated by the vibrational modes of the small cross-section fibres used in its construction. However, a useful pulse-echo response at 5 MHz was obtained from the transducer by filtering its output or by driving it in a narrow band mode. The ultrasonic pulse-echoes are broader than used for contemporary non destructive testing. This is appears to be a result of transducer ringing that could be reduced by the addition of a backing layer to the transducer fibres to dampen their resonant responses. This would be a valuable development of the flexible transducer that has not been attempted to date. A further development would be to cut the fibres into sets of short elements, perhaps 3 mm long, to provide flexibility in the direction normal to that achieved here.

Acknowledgement

The authors would like to acknowledge the Leverhulme Trust for funding this research (Grant F/00351/G).

References

[1] D.J. Powell, G. Hayward, Flexible ultrasonic transducer arrays for nondestructive evaluation applications, Part I: the theoretical modelling approach, IEEE Trans. Ultra. Ferro. Freq. Contrl. 43 (3) (1996) 385–391.

[2] D.J. Powell, G. Hayward, Flexible ultrasonic transducer arrays for nondestructive evaluation applications, Part II: performance assessment of different array configurations, IEEE Trans. Ultra. Ferro. Freq. Contrl. 43 (3) (1996) 393–402, 43(3), 393–402, 1996.

[3] A. Gachagan, P. Reynolds, G. Hayward, A. McNab, Construction and evaluation of a new generation of flexible ultrasonic transducers ultrasonics symposium, in: Proceedings 1996 IEEE, vol. 2, 3–6, 1996, pp. 853–856.

[4] A. Gachagan, P. Reynolds, G. Hayward, R. Monkhouse, P. Cawley, Piezoelectric materials for application in low profile interdigital transducer designs, ultrasonics symposium, IEEE, vol. 2, 5–8 October 1997, pp. 1025–1028.

[5] A. Gachagan, G. Hayward, R. Banks, A flexible piezoelectric transducer design for efficient generation and reception of ultrasonic lamb waves, IEEE Trans. Ultra. Ferro. Freq. Contrl. 52 (7) (2005) 1175–1182.

[6] D.J. Powell, G. Hayward, A performance appraisal of flexible array structures using a facet ensemble scattering technique, ultrasonics symposium, in: Proceedings IEEE, vol. 2, 8–11, 1991, pp. 753–756.

[7] E.K. Akdogan, M. Allahverdi, A. Safari, Piezoelectric composites for sensor and actuator applications, IEEE Trans. Ultra. Ferro. Freq. Contrl. 52 (5) (2005) 746–775.

[8] O. Roy, M.S. Chatillon, Ultrasonic inspection of complex geometry component specimen with a smart flexible contact phased array transducer: modeling and application, ultrasonics symposium, IEEE, vol. 1, 22–25 October 2000, pp. 763–766.

[9] S. Chatillon, G. Cattiaux, M. Serre, O. Roy, Ultrasonic nondestructive testing of pieces of complex geometry with a flexible phase array transducer, Ultrasonics 38 (2000) 131–134.

[10] O. Roy, S. Mahaut, O. Casula, Development of a smart flexible transducer to inspect component of complex geometry: modelling and experiment, CP615: review of quantitative nondestructive evaluation, vol. 21, in: D.O. Thompson, D.E. Chimenti (Eds.), Am. Inst. Phys. 2002, pp. 908–914.

[11] M. Kobayashi, Flexible ultrasonic transducers, IEEE Trans. Ultra. Ferro. Freq. Contrl. 53 (8) (2006) 1478–1486.

[12] F.S. Foster, K.A. Harasiewicz, M.D. Sherar, A history of medical and biological imaging with polyvinylidene fluoride (PVDF) transducers, IEEE Trans. Ultra. Ferro. Freq. Contrl. 47 (6) (2000) 1363–1371.

[13] Smart Material Corp., 31 Sarasota Center Blvd., Sarasota, FL 34240, USA.

[14] J.S. Sandhu, H. Wang, W.J. Popek, Acoustography for rapid inspection of composites, Proc. SPIE 2944, 117–120, 1996, Santec Systems Inc., Wheeling, IL 60090, USA. <www.santecsystems.com>.

[15] European Standard, EN 50324-2:2002. Piezoelectric properties of ceramic materials and components, Part 2: methods of measurement and properties – low power.

[16] D.A. Berlincourt, H.H.A. Krueger, C. Near, 1999 Properties of piezoelectric ceramics morgan electro ceramics technical, Publication 226, 1–12.

[17] L.J. Nelson, C.R. Bowen, R. Stevens, M. Cain, M. Stewart, Modelling and measurement of piezoelectric fibres and interdigitated electrodes for the optimisation of piezofibre composites smart structures and materials 2003: active materials: behaviour and mechanics, in: D.C. Lagoudas (Eds.), Proceedings of the Society of Photo-optical Instrumentation Engineers (SPIE) 5053 556-567, 2003, Smart Structures and Materials 2003 Conference, Sand Diego, CA, 2–6 March, 2003.

[18] D.A. Hall, Nonlinearity in piezoelectric ceramics, J. Mater. Sci. 36 (2001) 4575–4601.